Diagn Interv Radiol 2021; 27: 275–282

MODALITY-BASED (US, CT, MRI, PET-CT) IMAGING

ORIGINAL ARTICLE

A comparison study of dual-energy spectral CT and ^{18}F-FDG PET/CT in primary tumors and lymph nodes of lung cancer

Osman Kupik
Yavuz Metin
Gülnihan Eren
Nurgul Orhan Metin
Medeni Arpa

PURPOSE
We aimed to investigate whether there is a correlation between dual-energy spectral computed tomography (DESCT) and ^{18}F-fluorodeoxyglucose positron emission tomography/computed tomography (^{18}F-FDG PET/CT) parameters in primary tumor and metastatic lymph nodes in patients with newly diagnosed lung cancer.

METHODS
Primary tumor and metastatic lymph nodes of 68 patients diagnosed with lung cancer were evaluated retrospectively with ^{18}F-FDG PET/CT and DESCT imaging. The histologic subtypes were adenocarcinoma (n=29), squamous cell carcinoma (SCC) (n=26), small cell lung cancer (SCLC) (n=11), and large cell neuroendocrine cancer (LCNEC) (n=2). In terms of PET parameters, SUVmax, SUVmean, SULmax, SULmean, SULpeak, and normalized SUL values were obtained for primary tumors and metastatic lymph nodes. In terms of DESCT parameters, maximum and mean iodine content (IC), normalized IC values, iodine enhancement (IE) and normalized IE values were calculated.

RESULTS
We found no correlation between DESCT and ^{18}F-FDG PET/CT parameters in primary tumors and metastatic lymph nodes. In addition, no correlation was found in the analysis performed in any of the histologic subgroups. In patients with a primary tumor <3 cm, there was a moderate negative correlation between the parameters SUVmax-ICmax (r= -0.456, p = 0.043), SUVmean-ICmax (r= -0.464, p = 0.039) SULmean-ICmax (r= -0.497, p = 0.026), SUVmax-ICmean (r= -0.527, p = 0.020), SULmean-ICmean (r= -0.499, p = 0.025), and SULpeak-ICmean (r= -0.488, p = 0.029).

CONCLUSION
We consider that DESCT and ^{18}F-FDG PET/CT indicate different characteristics of the tumors and should not supersede each other.

Pretreatment imaging in lung cancer is valuable for determining the best strategy for the management of cancer therapy. ^{18}F-fluorodeoxyglucose positron emission tomography/computerized tomography (^{18}F-FDG PET/CT) has become a standard imaging technique for pulmonary nodule characterization (1). ^{18}F-FDG PET/CT is currently used for staging (2), planning therapy, restaging, therapeutic response assessment (3), and detection of recurrence. It has been revealed that maximum standardized uptake value (SUVmax) on ^{18}F-FDG PET/CT shows a significant correlation with tumor aggressiveness, thus SUVmax could be considered a predictor of response to treatment (4–6).

The dual-energy technique of a single-source computed tomographic (CT) scanning allows differentiation of iodine in the tissue due to its high photoelectric absorption. The dual-energy spectral CT (DESCT) provides a virtual unenhanced and an iodine-enhanced image from a single scanning after iodine contrast injection by differentiation of iodine content (IC) (7). DESCT-derived IC has been used for the differentiation of primary lung cancer (8, 9) and to discriminate benign from malignant pulmonary nodules (10–12). Iodine contents (mg/mL) estimated from DESCT were shown to be associated with the response to chemotherapy, and high iodine concentration was correlated to the treatment response of lung cancer (13). Although there is as yet insufficient evidence of DESCT

From the Departments of Nuclear Medicine (O.K. ✉ *osmankupik@gmail.com*), Radiation Oncology (G.E), Radiology (N.O.M.), and Biochemistry (M.A.), Recep Tayyip Erdoğan University School of Medicine, Rize, Turkey; Department of Radiology (Y.M.), Ankara University School of Medicine, Ibni Sina Hospital, Ankara, Turkey.

Received 03 February 2020; revision requested 25 February 2020; last revision received 15 April 2020; accepted 25 April 2020.

Published online 7 January 2021.

DOI 10.5152/dir.2021.20016

You may cite this article as: Kupik O, Metin Y, Eren G, Orhan Metin N, Arpa M. A comparison study of dual-energy spectral CT and ^{18}F-FDG PET/CT in primary tumors and lymph nodes of lung cancer. Diagn Interv Radiol 2021; 27: 275–282

for radiation therapy, DESCT-based IC has been shown to have a potential prognostic value for stereotactic body radiotherapy; tumors with lower iodine uptake had worse prognosis (14).

Some authors suggest that DESCT-based iodine quantitation might be an alternative to ^{18}F-FDG PET/CT in patients with NSCLC for the evaluation of response to chemotherapy/radiotherapy (15). Studies have shown that tumor perfusion was related to treatment response. The ratio of metabolism of the tumor assessed by ^{18}F-FDG PET/CT to perfusion obtained by dynamic CT, dynamic magnetic resonance imaging (MRI), or ^{15}O-water PET was reported to be associated with tumor recurrence; better perfused tumors showed better response to chemotherapy/radiotherapy, whereas patients whose tumors showed increased metabolism had earlier recurrence (16, 17). Recent studies reported that DESCT might represent tissue perfusion and therefore DESCT could have substantial clinical values. Calculating iodine enhancement (IE) by DESCT was proposed as a relatively simple method that might reflect the vascularization of the tumor tissue (18). The results of previous studies provide a foundation for further studies for the comparison of ^{18}F-FDG PET/CT and DESCT parameters in cancer tissue, including primary tumor and lymph nodes.

We aimed to investigate whether there was relation between DESCT and ^{18}F-FDG PET/CT parameters in primary tumor and metastatic lymph nodes in patients with lung cancer.

Methods

Study population

Newly diagnosed lung cancer patients who had pretreatment ^{18}F-FDG PET/CT and DESCT examinations between May 2016 and May 2017 were included. Sixty-eight patients (65 males, 3 females) aged between 48 and 87 years (median, 63.5 years) met our inclusion criteria. Twenty-nine patients (43%) had adenocarcinoma, 26 (38%) had squamous cell carcinoma (SCC), 11 (16%) had small cell lung cancer (SCLC), and 2 (3%) had large cell neuroendocrine cancer (LCNEC).

We could not obtain histopathologic confirmation for all lymph nodes because a small subgroup of patients underwent surgery. Regressing lymph nodes under treatment on follow-up imaging were accepted as metastatic. If there was no follow-up imaging, the decision was made through the consensus of a nuclear medicine specialist and two radiologists. When no consensus was reached, these lymph nodes were excluded from the study. In total, 143 metastatic thoracic lymph nodes were evaluated: 64 nodes with adenocarcinoma (44.8%), 42 nodes with SCC (29.4%), 34 nodes with SCLC (23.8%), 3 nodes with LCNEC (2.1%). There was a short period (0–23 days) between ^{18}F-FDG PET/CT and DESCT examinations to avoid significant changes in tumoral size and morphology. The period between the two imaging methods was considered adequate because a previous study reported no significant changes concerning tumor characteristics in less than 4 weeks (19). The Clinical Research Ethical Committee in Recep Tayyip Erdoğan University School of Medicine reviewed and approved this retrospective study (Decision number: 2019/03). As this was a retrospective study where the data was de-identified, it was exempt by the institutional review board from the need for informed consent.

DESCT imaging

All CT examinations were performed using the same CT scanner (Discovery CT750HD, GE Healthcare). Patients were injected with 80–100 mL (1.35 mL/kg of body weight) nonionic iodinated contrast material at a rate of 3.0–4.0 mL/s, and enhanced scans were obtained using the dual-energy spectral mode about 50 seconds after the injection of contrast agent. The scanning parameters for the GSI mode were: tube voltage, dynamic switching between 80 and 140 kVp within 0.5 ms; tube current between 275 and 640 mA; acquisitions were performed during a mid-inspiratory breath-hold.

The automatic reconstructions of iodine mapping and low keV virtual monochromatic images were performed on the Gemstone Spectral Imaging Viewer software on an independent advanced workstation (Advantage Workstation 2.0; GE Healthcare).

^{18}F-FDG PET/CT imaging

Patients with a serum glucose level of less than 180 mg/dL after at least 4 hours of fasting underwent 3.7 MBq/kg (0.1 mCi/kg) intravenous FDG injection. Images were taken (Biograph mCT; Siemens). A low-dose CT protocol was used for attenuation correction.

Image analysis of DESCT

DESCT data analysis was performed through consensus of two radiologists with 10 years of experience in thoracic imaging (Y.M., N.O.M). In each patient, the maximum and mean iodine contents of the primary tumor, metastatic lymphadenopathy, and ascending aorta were measured with three different circular regions of interest (ROIs) of the same size on the iodine mapping images. The mean value of the three different measurements was subsequently calculated and recorded. Normalized values were obtained by dividing iodine content values of tumors and metastatic lymphadenopathies to iodine content measurements of ascending aorta. With similar methods, IE values of primary tumors and metastatic lymph nodes were measured on 40 keV virtual monochromatic images (VMIs). Again, normalized values were obtained by dividing these values by the iodine enhancement values of ascending aorta on 40 keV VMI.

Image analysis of ^{18}F-FDG PET/CT

Each dataset was analyzed by nuclear medicine specialists with nine years of experience using a dedicated software application Syngo *via* MM Oncology (Siemens Healthcare). The maximum and mean standardized uptake value normalized to body mass (SUVmax, SUVmean), maximum and mean standardized uptake value normalized to lean body mass (SULmax, SULmean), SULpeak (corresponding to the highest possible mean value of a 1 cm^3 spherical volume of interest) were measured for the primary tumor and each lymph node. Blood pool (BP) SUVmean was measured in the ascending aorta.

We divided SUV measurements by BP SUVmean to obtain normalized SUV (nSUV) values and achieve standardization because SUV measurements are influenced by several factors such as patient weight, injected dose, glucose level, and uptake

Main points

- There was no statistically significant relation between ^{18}F-FDG PET/CT and DESCT parameters in lung cancer.
- ^{18}F-FDG PET/CT indicates glucose metabolism, whereas DESCT shows iodine concentration, which is an imaging technique used to reflect the vascularization/perfusion of tissue.
- In clinical practice, ^{18}F-FDG PET/CT and DESCT should not be preferred over one another.

time. Previous studies reported that either liver or mediastinal BP could be used to normalize SUV (19–21). Both methods have the disadvantage of being affected by several factors. On account of the fact that liver SUV normalization can be affected by steatosis (22), and the parameters in DESCT group were proportionated to the aorta (23) in our study, we used aorta BP for normalization of the SUV.

To confirm that the lesions at the same anatomic levels were measured on both DESCT and ^{18}F-FDG PET/CT, one nuclear medicine specialist and two radiologists performed simultaneous measurements. First, the most intensely FDG-enhancing area within each lesion was determined, then the same plane and same level was found on corresponding DESCT images and IC and IE values were obtained. Except for SULpeak, all PET measurements were performed by drawing ROIs. ROIs were drawn under the supervision of at least one nuclear medicine specialist and one radiologist, encompassing the lesion as much as possible. Necrotic areas were not included in the ROIs (Figs. 1, 2).

Statistical analysis

Descriptive statistics are given as mean ± standard deviation for variables with normal distribution, and median and interquartile range (IQR) for variables with non-normal distribution. In multiparametric groups, for nonparametric variables, the Kruskal-Wallis and Jonckheere-Terpstra tests were used, and for parametric variables, one-way analysis of variance (ANOVA) analysis was used to evaluate the difference between groups. If a *p* value less than 0.05 was found when comparing three histologic subgroups, Bonferroni correction was applied (*p* values lower than 0.017 were deemed as statistically significant); Student t test was used to compare parametric variables and Mann-Whitney U test for nonparametric variables. Correlation between groups was evaluated using Spearman correlation for non-parametric variables and the Pearson correlation coefficient for parametric variables. Also, the correlation of the parameters with the normalized values and the correlation between IC and IE (HU) of DESCT parameters were examined using both Pearson and Spearman correlation analyses.

We investigated the relationship between ICmean values of SCC and SCLC patients with Student t test. ROC analysis was performed to evaluate the discriminative value of significant parameters.

A statistical power analysis was performed for sample size estimation. The correlation ρ H1 in this study was 0.447 for 0.2 of coefficient of determination ρ2 with an alpha = 0.05 and power = 0.95. The sample size required for this correlation ρ H1 (GPower 3.1.9.2) was approximately n=59. Thus, our sample size of 68 was more than adequate for the main objective of this study.

Results

A total of 68 primary lung tumors (mean size 45.29±22.3 mm) in 68 patients were examined. The median and mean values of DESCT and ^{18}F-FDG PET/CT parameters for the entire group and the histologic subtypes are presented in Table 1. There was no statistically significant difference between the subgroups.

We found no relationship between IC and SUV or nIC and nSUV values of the primary tumors (ICmax-SUVmax r=0.133, p = 0.290; ICmean-SUVmean r=0.051, p = 0.687; ICmax-SULmax r=0.166, p = 0.187; ICmean-SULmean r=0.045, p = 0.724; ICmax-SULpeak r=0.146, p = 0.247; nICmax-nSUVmax r=0.022, p = 0.861; nICmean-SUVmean r=0.120, p = 0.342; nICmax- nSULpeak r=0.008, p = 0.953). There was no association between IE (HU) and SUVmax or SUVmean and normalized values of the primary tumors (IE-SUVmax

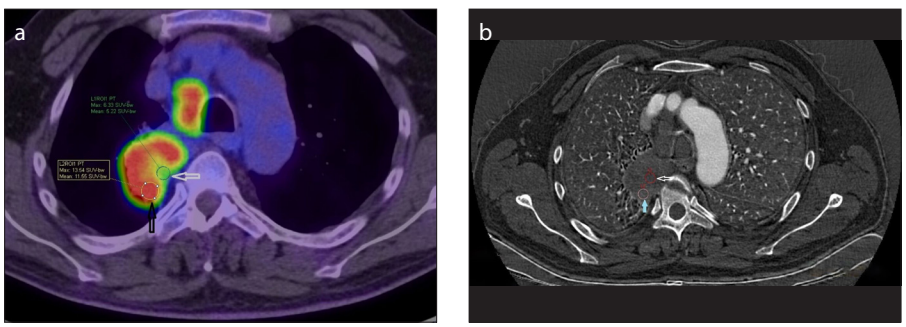

Figure 1. a, b. Transaxial ^{18}F-FDG PET/CT fusion image **(a)** and transaxial iodine mapping image **(b)** show a 62-year-old man with right lung adenocarcinoma; simultaneous measurements were taken from the posterior viable portion of the tumor. The axial cross-section with the most intense FDG uptake was determined and a ROI was drawn on the fusion image of ^{18}F-FDG PET/CT (**a,** *black arrow*) and a ROI with the same size was drawn around the same cross-section on the DESCT (**b,** *blue arrow*; ICmean, 11.02 mg/mL) and measurements were recorded. The necrotic region with a low FDG-uptake was observed in the medial side of the central portion of the tumor; this region was not included in the evaluation (**a**, *white arrow*, SUVmax, 5.2; **b,** *white arrow*, ICmean, 3.3 mg/mL).

Figure 2. a–c. Transaxial ^{18}F-FDG PET/CT fusion image **(a)**, transaxial 40 keV virtual monochromatic image **(b)**, and transaxial iodine mapping image **(c)** show a 58-year-old man with adenocarcinoma. A ROI (1.27 cm^2) with the highest FDG uptake was drawn around right paratracheal lymph node on the ^{18}F-FDG PET/CT; SUVmax, 11.5 and SUVmean, 10.9 (**a,** *black arrow*). ROIs with approximately similar size (1.34 cm^2) were obtained on the same axial section of DESCT, which revealed IE, 137 HU (**b,** *black arrow*) and ICmean, 14.3 mg/mL (**c,** *black arrow*).

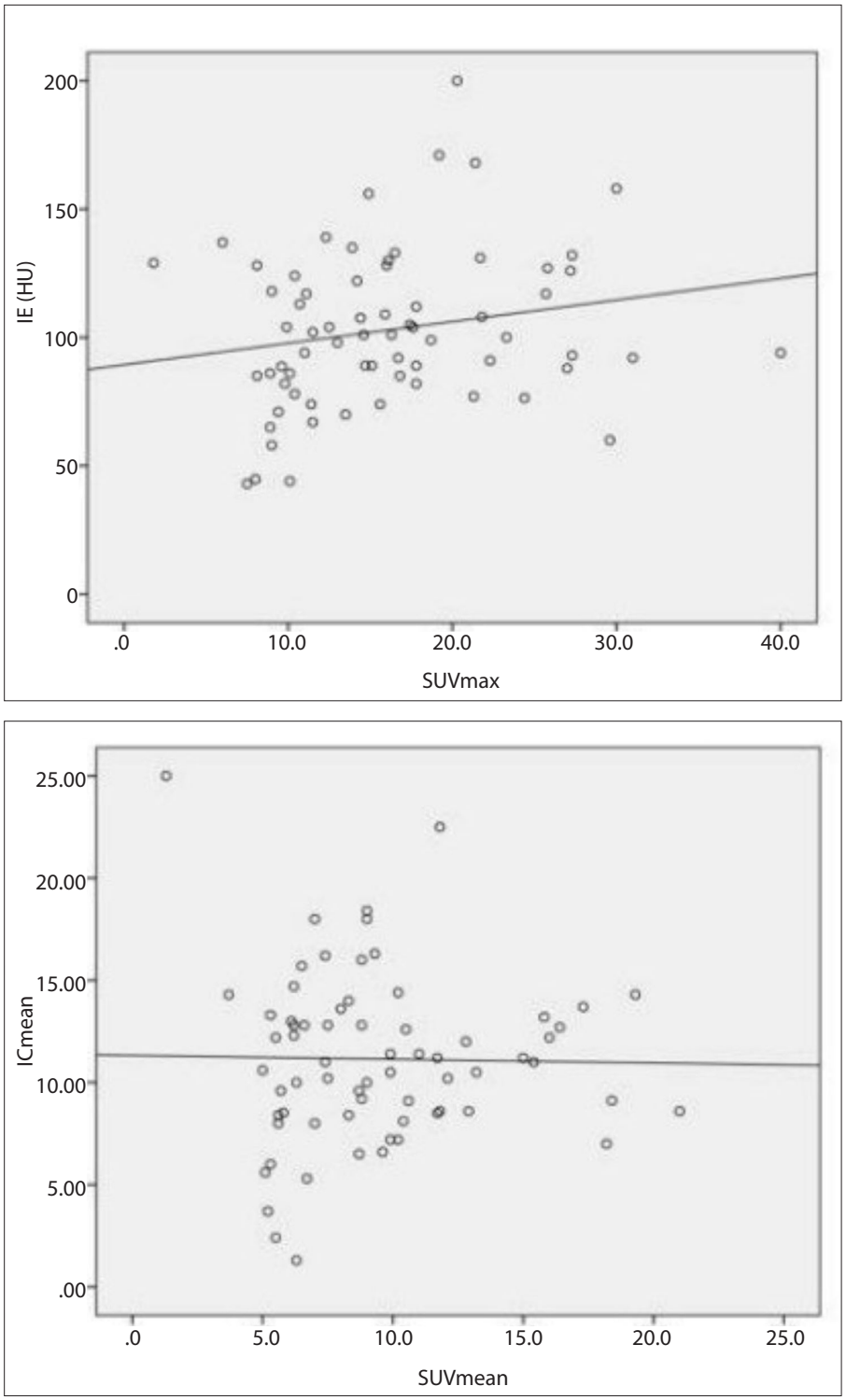

Figure 3. A scatterplot of the analysis of primary tumors (n=68) revealed no correlation between DESCT and ^{18}F-FDG PET/CT parameters.

r=0.238, p = 0.056; IE-SUVmean r=0.240, p = 0.054; nIE-nSUVmax r=0.119, p = 0.344; nIE-nSUVmean r=0.109, p = 0.389; nIE-nSULpeak r=0.177, p = 0.158) (Fig. 3). A weak statistical correlation was observed between IE (HU) and SULmean (r=0.255, p = 0.041) or SULpeak (r=0.271, p = 0.029) and SULmax (r=0.258, p = 0.038) values of the primary tumors (Table 2).

There was no statistically significant correlation between the parameters even when the analysis of the tumors was grouped according to tumor histologic subtypes (p > 0.05).

We observed a statistically significant difference between SCC and SCLC only in terms of ICmean values among DESCT parameters (SCC, 11.18±3.75 vs. SCLC, 8.5±3.02; p = 0.043). The distinctive value of ICmean for SCC and SCLC was determined by ROC analysis (area under curve [AUC)]= 0.704, p = 0.036). ICmean threshold set at 10.1 mg/mL yielded 69% sensitivity and 77% specificity.

There were 20 patients (29.4%) with a tumor size <3 cm and 48 patients (70.6%) with a tumor size ≥3 cm. There was no correlation between IC/IE and SUV/SUL in the group with a tumor size ≥3 cm: SUVmax vs. ICmax, r=0.219, p = 0.135; SUVmean vs. ICmean, r=0.212, p = 149; SULpeak vs. ICmean, r=0.217, p = 0.139; SUVmean vs. IE, r=0.238, p = 0.103. However, there was a moderate negative correlation between the parameters in the group with a tumor size of <3 cm: SUVmax vs. ICmax, r= -0.456, p = 0.043; SUVmean vs. ICmax, r= -0.464, p = 0.039; SULmean vs. ICmax, r= -0.497, p = 0.026; SUVmax vs. ICmean, r= -0.527, p = 0.020; SULmean vs. ICmean, r= -0.499, p = 0.025; SULpeak vs. ICmean, r= -0.488, p = 0.029.

Three lymph nodes diagnosed as LCNEC were excluded from the study. Totally, 140 lymph nodes were included in the study (median size, 15; range, 7–43 mm). No correlation was found between IC/IE and SUV/SUL or normalized parameters in the entire group: ICmax vs. SUVmax, r=0.064, p = 0.453; ICmean vs. SUVmean, r=0.150, p = 0.076; ICmean vs. SULpeak, r=0.045, p = 0.601; IE vs. SULpeak, r=0.122, p = 0.150; nICmax vs. nSUVmax, r=0.029, p = 0.731, nICmean vs. SUVmean, r=0.040, p = 0.641; nICmean vs. nSULpeak r=0.024, p = 0.783; nIE vs. nSULpeak, r=0.032, p = 0.708. The correlation summary of lymph nodes is given in Table 3.

The analysis of histologic subgroups revealed no statistically significant (p > 0.05) correlation between DESCT and ^{18}F-FDG PET/CT parameters. Nevertheless, ^{18}F-FDG PET/CT and DESCT parameters of lymph nodes in SCC were found to be higher than in the other histologic subgroups (Table 4, Fig. 4).

We observed a good correlation in DESCT and ^{18}F-FDG PET/CT parameters of the patients with normalized values: SUVmax, r=0.863, p < 0.001; SULmax, r=0.889, p < 0.001; SUVmean, r=0.849, p < 0.001; SULmean, r=0.857, p < 0.001; SULpeak, r=0.903, p < 0.001; ICmax, r=0.719, p < 0.001; ICmean, r=0.761, p < 0.001; IE (HU), r=0.534, p < 0.001.

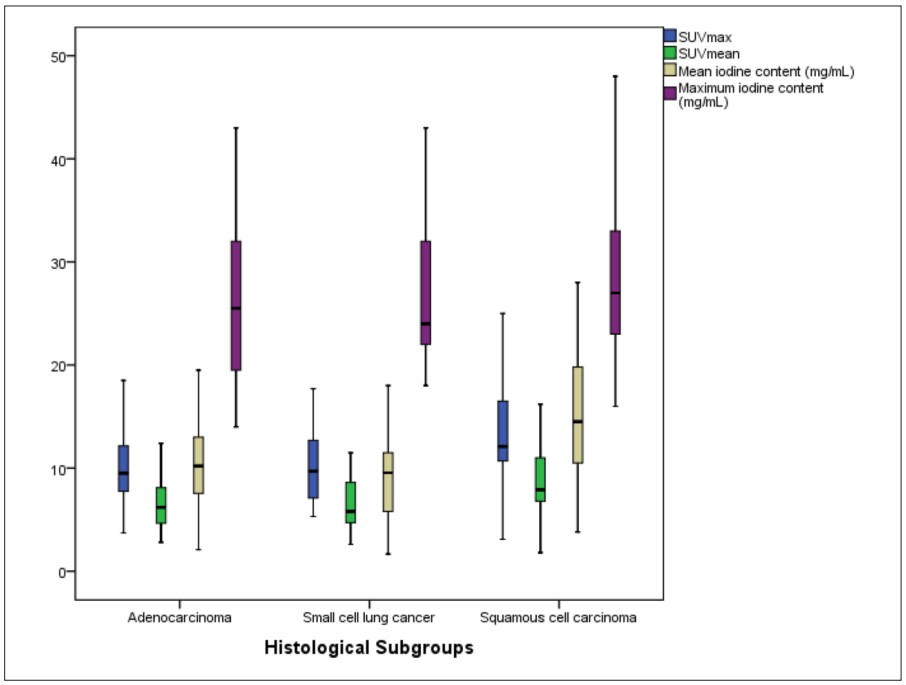

Figure 4. A boxplot of SUVmax, SUVmean, ICmax, and ICmean of lymph nodes for patients with adenocarcinoma, SCLC, and SCC. DESCT and ^{18}F-FDG PET/CT parameters were found to be higher in histologic subgroup of SCC compared with others.

Table 1. Mean and median values of primary tumor for all group and histologic subgroups

	All patients	Adenocarcinoma	SCC	SCLC	
	Median (IQR)/ Mean±SD	Median (IQR)/ Mean±SD	Median (IQR)/ Mean±SD	Median (IQR)/ Mean±SD	*p*
SUVmax	15 (10.7)	15±6.66	18.19±6.63	11.5 (7.8)	0.133
SUVmean	8.8 (5.5)	8.65±3.68	10.79±4.16	7.4 (4.9)	0.108
SULmax	11.7 (8.3)	11.7±5.55	16.83±13.98	8.3 (6.9)	0.079
SULmean	6.8 (4.3)	6.71±3.12	8.45±3.40	5.3 (4.5)	0.052
SULpeak	10.1±5.1	9.1 (7.2)	11.1±4.46	7.4 (5.5)	0.517
ICmax (mg/mL)	29.59±7.86	30.59±7.99	29.08±7.46	22.27±5.23	0.433
ICmean (mg/mL)	11.14±4.17	11.99±4.51	11.3 (4.63)	8.5±3.02	0.056
IE (HU)	102.96±30.48	105.66±29.79	105.62±33.63	88.68±23.38	0.250

There was no statistically significant difference between subgroups.
SCC, squamous cell carcinoma; SCLC, small cell lung cancer; IQR, interquartile range; SD, standard deviation; SUV, standardized uptake value; SUL, standardized uptake value normalized by lean body mass; IC, iodine content; IE, iodine enhancement; HU, Hounsfield unit.

IC and IE (HU) values of the patients showed a good correlation: ICmean vs. IE, r=0.768, $p < 0.001$; nICmean vs. nIE, r=0.710, $p < 0.001$; ICmax vs. IE, r=0.500, $p < 0.001$; and nICmax vs. nIE, r=0.705, $p < 0.001$.

Discussion

In this study, we found that there was no correlation between DESCT and ^{18}F-FDG PET/CT parameters in the primary tumors of lung cancer and the lymph nodes evaluated as metastatic, and also in the histological subtypes of the lung cancer. In the literature, some studies reported results that may be interpreted contrary to the results of our study, while others supported our findings and found no correlation between the groups.

In a study conducted in 37 patients with lung cancer, authors reported various degrees of correlation between IEmax and SUVmax values in the primary tumor and lymph nodes (24). The authors suggested that the late progress in tumor molecular genetics might provide rational biologic grounds for the association of these two parameters, and exemplified the p53 oncogene, which is a promoter of tumor angiogenesis and metabolism and is frequently expressed in lung cancer. In the study by Baxa et al. (18) metabolic volume-based ^{18}F-FDG PET/CT parameters and DESCT parameters were compared in 48 patients with NSCLC. The study reported that there was no correlation or a negative correlation between IE (HU) and SUV, albeit a weak-moderate degree of relationship between total IC and SUVmax, SUVmean, and SUVpeak values. Total IC was compared with metabolic tumor volume (MTV) and total lesion glycolysis (TLG) in their study. However, MTV demonstrates viable tissue volume. There would be no FDG accumulation in this region and this tissue would be exclud-

Table 2. The summary of correlation of the DESCT and 18F-FDG PET/CT parameters in the primary tumor

	SUVmax		SUL max		SULpeak		SUVmean		SULmean			nSUVmax		nSULpeak		nSUVmean	
	r	*p*	r	*p*	r	*p*	r	*p*	r	*p*	nICmax	r	*p*	r	*p*	r	*p*
ICmax (mg/mL)	0.133	0.290	0.166	0.187	0.146	0.247	-	-	-	-		- 0.022	0.861	- 0.008	0.953	-	-
ICmean (mg/mL)	-	-	-	-	0.026	0.834	0.051	0.687	0.045	0.724	nICmean	-	-	-0.110	0.382	-0.120	0.342
IE (HU)	0.238	0.056	0.258	0.038*	0.271	0.029*	0.240	0.054	0.255	0.041*	nIE(HU)	0.119	0.344	0.177	0.158	0.109	0.389

A statistically significant, albeit low, correlation between IE and SULmax, SULpeak and SULmean was observed. The empty boxes were due to the comparison of SUV/SULmax with ICmean. SULpeak values were compared both with ICmax and ICmean.
SUV, standardized uptake value, SUL, standardized uptake value normalized by lean body mass; IC, iodine content; IE, iodine enhancement; HU, Hounsfield unit.
*Statistically significant.

Table 3. The summary of correlation analysis of the parameters in the lymph nodes

	SUVmax		SULmax		SULpeak		SUVmean		SULmean			nSUVmax		nSULmax		nSULpeak		nSUVmean		nSULmean	
	r	*p*	r	*p*	r	*p*	r	*p*	r	*p*		r	*p*	r	*p*	r	*p*	r	*p*	r	*p*
ICmax (mg/mL)	0.064	0.453	0.025	0.767	-0.015	0.856	-	-	-	-	nICmax	-0.029	0.731	0.100	239	-0.059	0.485	-	-	-	-
ICmean (mg/mL)	-	-	-	-	0.045	0.601	0.150	0.076	0.128	0.131	nICmean	-	-	-	-	-0.024	0.783	0.040	0.641	-0.020	0.812
IE(HU)	0.179	0.034	0.173	0.041	0.122	0.150	0.157	0.064	0.146	0.085	nIE(HU)	0.071	0.403	0.045	0.602	0.032	0.708	0.049	0.568	0.012	0.892

There was no statistically significant correlation between the parameters. The empty boxes were due to the comparison of SUV/SULmax with ICmean. SULpeak values were compared both with ICmax and ICmean.
SUV, standardized uptake value, SUL, standardized uptake value normalized by lean body mass; IC, iodine content; IE, iodine enhancement; HU, Hounsfield unit.

Table 4. Mean and median values in histologic subgroups of lymph nodes

	Adenocarcinoma (n=64)	SCLC (n=34)	SCC (n=42)	
	Median (IQR)/ Mean±SD	Median (IQR)/ Mean±SD	Median (IQR)/ Mean±SD	*p*
IE (HU)	109.19±41.56	89 (56)	143.5±63.13	0.004[a]; <0.001[b]
ICmax (mg/mL)	26.1±7	26.88 (10.5)	28.5±6.91	0.189
ICmean (mg/mL)	10.87±4.65	9.4±4.81	15.1±6.87	0.001[a,b]
SULmax	7.4 (3.5)	6.85 (3.9)	9.5 (4.7)	0.001[a,b]
SULmean	4.75 (2.6)	5.1 (2.6)	6.35 (3.2)	0.001[a,b]
SULpeak	5.6 (2.8)	6.5 (3.1)	7.85 (4.7)	0.002[a]; 0.009[b]
SUVmax	9.5 (4.5)	9.7 (5.7)	12.1 (6)	0.001[a]; 0.009[b]
SUVmean	6.2 (3.6)	5.8 (4)	7.9 (4.7)	0.001[a]; 0.008[b]

In patients with SCC, all parameters, except ICmax, were significantly higher than in patients with adenocarcinoma and SCLC.
SCLC, small cell lung cancer; SCC, squamous cell carcinoma; IQR, interquartile range; SD, standard deviation; IE, iodine enhancement; HU, Hounsfield unit; IC, iodine content; SUL, standardized uptake value normalized by lean body mass; SUV, standardized uptake value.
[a]*p* value for adenocarcinoma vs. SCC in post hoc analysis; [b]*p* value for SCLC vs. SCC in post hoc analysis.

ed in MTV because the necrotic component of the tumor would not have a metabolic activity. Also, iodine-based contrast agents would not accumulate in the necrotic tissue. Thus, the positive correlation between MTV and total iodine content is not an unexpected result. The authors emphasized that lowering the SUV threshold increases the correlation coefficient, which also leads to values that are closer to the true volume of the tumor, namely the volume of the tumor measured on CT. In our study we did not include MTV and TLG; we use them to determine disease prognosis (25).

Aoki et al. (26) investigated the correlation between average iodine density (AID) obtained by DESCT and SUVmax values in 74 patients with NSCLC who underwent stereotactic body radiation therapy. The study revealed no significant correlation between these two parameters. Moreover, they observed a significantly negative impact of tumors with a lower AID and higher SUVmax on local control. The study of Iwano et al. (27) which evaluated 62 primary tumors of 60 patients and compared tumor grade and iodine volume, revealed that higher grade tumors had smaller volumes of iodine in comparison with lower grade tumors. The ^{18}F-FDG PET/CT scan of 43% (n=27) were available in this study, and a negative correlation of delayed iodine volume with SUVmax was reported (r= -0.594, $p < 0.001$); however, no statistically significant relationship was found between arterial phase iodine volume and SUV (r= -0.297, $p = 0.088$).

Van Elmpt et al. (28) compared ^{18}F-FDG PET/CT and DESCT parameters in 33 patients with NSCLC and reported that neither modality had a relationship. They emphasized that DESCT might contribute to the characterization of NSCLC with ^{18}F-FDG PET/CT. In our study, we evaluated SUV normalized to lean body mass (SULmax, SULmean, and SULpeak), which, to our knowledge, have not been well studied before. In a study of patients with breast carcinoma who had not yet received therapy, the relationship between perfusion and metabolism was evaluated using a dual radiotracer, and a strong correlation of SUL with perfusion was reported (r=0.82, $p = 0.007$) (29). In our study, we found a statistically significant, albeit poor correlation between IE and SULmean (r= 0.255, $p = 0.041$), SULpeak (r= 0.271, $p = 0.029$), and SULmax (r= 0.258, $p = 0.038$). Taking into consideration the findings of Zasadny et al. (29), who showed a relationship with SUL, we suppose that this result is the indirect manifestation of the concordance of DESCT parameters and their ability to reflect tissue perfusion.

Although studies that compared DESCT with ^{18}F-FDG PET/CT have not grouped patients according to tumor size, Tateishi et al. (30) studied the relationship between peak attenuation (Apa) and relative flow (RF) with SUV in patients with NSCLC (tumor size, 2.6±0.2 cm; range, 0.9–3.4 cm) and showed that both perfusion parameters of CT had a correlation with SUV (Apa vs. SUV, r=0.665; RF vs. SUV, r=0.848; $p < 0.001$ for both). Miles et al. (31) compared standardized perfusion value (SPV) with SUV in 18 patients with NSCLC, and reported that there was no correlation for the whole group (n=18); although there was a statistically significant relation in patients with tumor size <4.5 cm^2 (n=6, mean size 2.4 cm). The authors discussed that the tumor perfusion and tumor metabolism relationship was related with tumor size, biologic aspects of tumor differentiate as it becomes larger, and the metabolic-perfusion difference is more prominent in large and high-grade tumors. Likewise, we divided patients into two groups according to tumor size, and we accepted 3 cm as a threshold. The analysis of primary tumors according to tumor size showed moderate negative correlations of the parameters in the group with tumor size <3 cm (n=20), and we consider that

with a larger sample size the correlation might have been stronger.

Lymph node analysis in our study revealed no correlation between DESCT and ^{18}F-FDG PET/CT parameters for the whole group or the histologic subgroups. To our knowledge, our study has the largest sample group with similar data analysis of the metastatic lymph nodes of lung cancer in the literature (n=140). Nevertheless, a study that evaluated 86 metastatic lymph nodes of lung cancer reported a moderate correlation between DESCT and ^{18}F-FDG PET/CT parameters (24). The authors accepted lymph nodes with a SUVmax above 2.5 as metastatic, but in our everyday clinical practice, we usually encounter lymph nodes with a relatively high FDG uptake without malignancy. In our study, a considerable number of lymph nodes had a SUVmax above 2.5, but they were excluded from the study by expert consensus. Although we did not find any relation between DESCT and ^{18}F-FDG PET/CT parameters, we observed a statistically significant difference between the subgroups, SUV parameters, ICmean, and IE (HU) values of lymph nodes were statistically significantly higher in the subgroup with SCC (Fig. 4). To the best of our knowledge, no previous study compared DESCT parameters among the histologic subgroups.

In recent studies, it was reported that DESCT might reflect tissue perfusion, and this reflection had a significant clinical impact. The authors suggested that a DESCT parameter, IE, could provide a relatively simple method to represent tumor vascularization (18). Some authors emphasized that DESCT, representing the exact iodine content in tumor tissue, could be used as an alternative to dynamic imaging modalities (32). Li et al. (33) concluded that DESCT-obtained iodine-related attenuation (IRA) could be used to determine the perfusion parameters of malignant tissue and tumor vascularization. Stiller et al. (34) reported a strong correlation between CT perfusion (mL/100 mL/min) and IC (mg/mL) obtained by DESCT in 24 patients with pancreas cancer (r=0.89). A study indicated that DESCT might have been used as an imaging method to assess tumor angiogenesis because iodine distribution in tissue is strongly related to local blood volume and vascular intensity (7, 24). In a study, Kim et al. (35) discussed that DESCT could be used to evaluate chemotherapy response and might differentiate intratumoral hemorrhage from actual enlargement of the tumor tissue. Also, DESCT-based iodine quantifications were shown to be useful in the evaluation of anti-EGFR treatment response (36). In another study, IRA in DESCT was reported to be a reliable parameter for evaluating antiangiogenic chemotherapy response in patients with advanced stage lung cancer (35). Moreover, DESCT-based IC was shown to be more reliable than HU and response evaluation criteria in solid tumors (RESIST) for patients with adenocarcinoma in predicting treatment response (13).

Ito et al. (37) investigated the role of DESCT and ^{18}F-FDG PET/CT for histopathologic invasiveness in 63 patients with NSCLC and reported that the ratio calculated from arterial and delayed-phase (A/D) DESCT was related to pathologic tumor invasiveness, as well as SUVmax on ^{18}F-FDG PET/CT. Also, they emphasized that for small lung tumors, the A/D ratio might be superior to SUVmax for the prediction of tumor invasiveness. Several studies conducted on metabolism and perfusion relationship of tumors indicated that this association might contribute to therapy management and could predict prognosis. A study that was conducted in patients with breast cancer revealed that although chemotherapy-related metabolism decreases, perfusion might not decrease, but rather increase (38). Moreover, PSA response was found to be correlated with glucose metabolism and inversely related to perfusion changes in patients with thalidomide-treated androgen-independent prostate cancer (39). Herbst et al. (40) evaluated high-dose endostatin (an antivascular agent) response in 25 patients and reported that perfusion calculated by ^{15}O-water PET/CT decreased, yet glucose metabolism in ^{18}F-FDG PET had been increasing.

Possibly, the measurement of tissue perfusion in DESCT might contribute to cancer treatment management when used in conjunction with ^{18}F-FDG PET/CT, which represents tumor metabolism (41), because DESCT is less expensive and/or has a lower radiation dose than most of the other radiologic modalities.

This study has some limitations. Our patients may be considered as a heterogeneous group. The patients except those with NSCLC might have been excluded; however, in subgroup analysis, we still observed no correlation, hence including SCLC and LNEC patients did not affect the results, also we had the chance to analyze the subgroup of patients with SCLC. Only 3 of 68 patients were women in our study. The most important reason for the male predominance may be that this was a single-center study and in this country and region, the frequency of smoking in women is very low, so lung cancer is relatively uncommon in the female population. We considered evaluating the prognostic value of the parameters of both modalities, DESCT and ^{18}F-FDG PET/CT, when used together. However, the therapy protocols of the patients could not be standardized; some patients declined therapy, some declined therapy options, and some were lost to follow-up. Therefore, our results might have been incorrect or biased if we performed survival analyses.

In conclusion, there was no relation between DESCT and ^{18}F-FDG PET/CT parameters of primary tumors and metastatic lymph nodes in lung cancer. ^{18}F-FDG PET/CT indicates tumor metabolism, whereas DESCT shows iodine concentration, which is an approved imaging technique used to reflect the vascularization/perfusion of tissue. In clinical practice, these two modalities should not be preferred over one another.

Conflict of interest disclosure

The authors declared no conflicts of interest.

References

1. Ruilong Z, Daohai X, Li G, Xiaohong W, Chunjie W, Lei T. Diagnostic value of 18F-FDG-PET/CT for the evaluation of solitary pulmonary nodules: a systematic review and meta-analysis. Nucl Med Commun 2017; 38:67–75. [Crossref]
2. Huellner MW, de Galiza Barbosa F, Husmann L, et al. TNM staging of non–small cell lung cancer: comparison of PET/MR and PET/CT. J Nucl Med 2016; 57:21–26. [Crossref]
3. Hicks RJ. Role of 18F-FDG PET in assessment of response in non–small cell lung cancer. J Nucl Med 2009; 50:31–42. [Crossref]
4. Lee DS, Kim YS, Yoo IR, et al. Long-term clinical experience of high-dose ablative lung radiotherapy: high pre-treatment [18F] fluorodeoxyglucose-positron emission tomography maximal standardized uptake value of the primary tumor adversely affects treatment outcome. Lung Cancer 2013; 80:172–178. [Crossref]
5. Takeda A, Yokosuka N, Ohashi T, et al. The maximum standardized uptake value (SUVmax) on FDG-PET is a strong predictor of local recurrence for localized non-small-cell lung cancer after stereotactic body radiotherapy (SBRT). Radiother Oncol 2011; 101:291–297. [Crossref]
6. Kohutek ZA, Wu AJ, Zhang Z, et al. FDG-PET maximum standardized uptake value is prognostic for recurrence and survival after stereotactic body radiotherapy for non-small cell lung cancer. Lung Cancer 2015; 89:115–120. [Crossref]

7. Chae EJ, Song J-W, Seo JB, Krauss B, Jang YM, Song K-S. Clinical utility of dual-energy CT in the evaluation of solitary pulmonary nodules: initial experience. Radiology 2008; 249:671–681. [Crossref]
8. Son JY, Lee HY, Kim J-H, et al. Quantitative CT analysis of pulmonary ground-glass opacity nodules for distinguishing invasive adenocarcinoma from non-invasive or minimally invasive adenocarcinoma: the added value of using iodine mapping. Eur Radiol 2016; 26:43–54. [Crossref]
9. Wang G, Zhang C, Li M, Deng K, Li W. Preliminary application of high-definition computed tomographic Gemstone Spectral Imaging in lung cancer. J Comput Assist Tomogr 2014; 38:77–81. [Crossref]
10. Zhang Y, Cheng J, Hua X, et al. Can spectral CT imaging improve the differentiation between malignant and benign solitary pulmonary nodules? PLoS One 2016; 11:e0147537. [Crossref]
11. Altenbernd J, Wetter A, Umutlu L, et al. Dual-energy computed tomography for evaluation of pulmonary nodules with emphasis on metastatic lesions. Acta Radiol 2016; 57:437–443. [Crossref]
12. Chae EJ, Song J-W, Krauss B, et al. Dual-energy computed tomography characterization of solitary pulmonary nodules. J Thorac Imaging 2010; 25:301–310. [Crossref]
13. Hong SR, Hur J, Moon YW, et al. Predictive factors for treatment response using dual-energy computed tomography in patients with advanced lung adenocarcinoma. Eur J Radiol 2018; 101:118–123. [Crossref]
14. Aoki M, Hirose K, Sato M, et al. Prognostic impact of average iodine density assessed by dual-energy spectral imaging for predicting lung tumor recurrence after stereotactic body radiotherapy. J Radiat Res 2016; 57:381–386. [Crossref]
15. Ren Y, Jiao Y, Ge W, et al. Dual-energy computed tomography–based iodine quantitation for response evaluation of lung cancers to chemoradiotherapy/radiotherapy: a comparison with fluorine-18 fluorodeoxyglucose positron emission tomography/computed tomography–based positron emission tomography/computed tomography response evaluation criterion in solid tumors. J Comput Assist Tomogr 2018; 42:614–622. [Crossref]
16. Mankoff DA, Dunnwald LK, Partridge SC, Specht JM. Blood flow-metabolism mismatch: good for the tumor, bad for the patient. Clin Cancer Res 2009; 15:5294–5296. [Crossref]
17. Dunnwald LK, Gralow JR, Ellis GK, et al. Tumor metabolism and blood flow changes by positron emission tomography: relation to survival in patients treated with neoadjuvant chemotherapy for locally advanced breast cancer. J Clinical Oncol 2008; 26:4449. [Crossref]
18. Baxa J, Matouskova T, Ludvik J, et al. Single-source dual-energy CT as a part of 18F-FDG PET/CT: direct comparison of iodine-related and metabolic parameters in non-small cell lung cancer. Anticancer Res 2018; 38:4131–4137. [Crossref]
19. Shanbhogue AKP, Karnad AB, Prasad SR. Tumor response evaluation in oncology: current update. J Comput Assist Tomogr 2010; 34:479–484. [Crossref]
20. Boktor RR, Walker G, Stacey R, Gledhill S, Pitman AG. Reference range for intrapatient variability in blood-pool and liver SUV for 18F-FDG PET. J Nucl Med 2013; 54:677–682. [Crossref]
21. Kim SJ, Yi HK, Lim CH, et al. Intra-patient variability of FDG standardized uptake values in mediastinal blood pool, liver, and myocardium during R-CHOP chemotherapy in patients with diffuse large B-cell lymphoma. Nuclear Med Mol Imaging 2016; 50:300–307. [Crossref]
22. Abikhzer G, Alabed YZ, Azoulay L, Assayag J, Rush C. Altered hepatic metabolic activity in patients with hepatic steatosis on FDG PET/CT. AJR Am J Roentgenol 2011; 196:176–180. [Crossref]
23. Patel BN, Vernuccio F, Meyer M, et al. Dual-energy CT material density iodine quantification for distinguishing vascular from nonvascular renal lesions: normalization reduces Intermanufacturer threshold variability. AJR Am J Roentgenol 2019; 212:366–376. [Crossref]
24. Schmid-Bindert G, Henzler T, Chu T, et al. Functional imaging of lung cancer using dual energy CT: how does iodine related attenuation correlate with standardized uptake value of 18FDG-PET-CT? Eur Radiol 2012; 22:93–103. [Crossref]
25. Liao S, Penney BC, Wroblewski K, et al. Prognostic value of metabolic tumor burden on 18 F-FDG PET in nonsurgical patients with non-small cell lung cancer. Eur J Nucl Med Mol Imaging 2012; 39:27–38. [Crossref]
26. Aoki M, Akimoto H, Sato M, et al. Impact of pretreatment whole-tumor perfusion computed tomography and 18F-fluorodeoxyglucose positron emission tomography/computed tomography measurements on local control of non–small cell lung cancer treated with stereotactic body radiotherapy. J Radiat Res 2016; 57:533–540. [Crossref]
27. Iwano S, Ito R, Umakoshi H, Ito S, Naganawa S. Evaluation of lung cancer by enhanced dual-energy CT: association between three-dimensional iodine concentration and tumour differentiation. Br J Radiol 2015; 88:20150224. [Crossref]
28. van Elmpt W, Das M, Hüllner M, et al. Characterization of tumor heterogeneity using dynamic contrast enhanced CT and FDG-PET in non-small cell lung cancer. Radiother Oncol 2013; 109:65–70. [Crossref]
29. Zasadny KR, Tatsumi M, Wahl RL. FDG metabolism and uptake versus blood flow in women with untreated primary breast cancers. Eur J Nucl Med Mol Imaging 2003; 30:274–280. [Crossref]
30. Tateishi U, Nishihara H, Tsukamoto E, Morikawa T, Tamaki N, Miyasaka K. Lung tumors evaluated with FDG-PET and dynamic CT: the relationship between vascular density and glucose metabolism. J Comput Assist Tomogr 2002; 26:185–190. [Crossref]
31. Miles K, Griffiths M, Keith C. Blood flow–metabolic relationships are dependent on tumour size in non-small cell lung cancer: a study using quantitative contrast-enhanced computer tomography and positron emission tomography. Eur J Nucl Med Mol Imaging 2006; 33:22–28. [Crossref]
32. Zhang LJ, Yang GF, Wu SY, Xu J, Lu GM, Schoepf UJ. Dual-energy CT imaging of thoracic malignancies. Cancer Imaging 2013; 81. [Crossref]
33. Li X, Meng X, Ye Z. Iodine quantification to characterize primary lesions, metastatic and non-metastatic lymph nodes in lung cancers by dual energy computed tomography: an initial experience. Eur J Radiol 2016; 85:1219–1223. [Crossref]
34. Stiller W, Skornitzke S, Fritz F, et al. Correlation of quantitative dual-energy computed tomography iodine maps and abdominal computed tomography perfusion measurements: are single-acquisition dual-energy computed tomography iodine maps more than a reduced-dose surrogate of conventional computed tomography perfusion? Invest Radiol 2015; 50:703–708. [Crossref]
35. Kim YN, Lee HY, Lee KS, et al. Dual-energy CT in patients treated with anti-angiogenic agents for non-small cell lung cancer: new method of monitoring tumor response? Korean J Radiol 2012; 13:702–710. [Crossref]
36. Baxa J, Matouskova T, Krakorova G, et al. Dual-phase dual-energy CT in patients treated with erlotinib for advanced non-small cell lung cancer: possible benefits of iodine quantification in response assessment. Eur Radiol 2016; 26:2828–2836. [Crossref]
37. Ito R, Iwano S, Shimamoto H, et al. A comparative analysis of dual-phase dual-energy CT and FDG-PET/CT for the prediction of histopathological invasiveness of non-small cell lung cancer. Eur J Radiol 2017; 95:186–191. [Crossref]
38. Mankoff DA, Dunnwald LK, Gralow JR, et al. Changes in blood flow and metabolism in locally advanced breast cancer treated with neoadjuvant chemotherapy. J Nucl Med 2003; 44:1806–1814.
39. Kurdziel KA, Figg WD, Carrasquillo JA, et al. Using positron emission tomography 2-deoxy-2-[18F] fluoro-D-glucose, 11CO, and 15O-water for monitoring androgen independent prostate cancer. Mol Imaging Biol 2003; 5:86–93. [Crossref]
40. Herbst RS, Mullani NA, Davis DW, et al. Development of biologic markers of response and assessment of antiangiogenic activity in a clinical trial of human recombinant endostatin. J Clin Oncol 2002; 20:3804–3814. [Crossref]
41. Li X, Du Y, Ma Y, Postel G, Civelek A. 18F-fluorodeoxyglucose uptake and tumor hypoxia: Revisit 18F-fluorodeoxyglucose in oncology application. Transl Oncol 2014; 7:240–247. [Crossref]